The 6th ASME-JSME Thermal Engineering Joint Conference
March 16-20, 2003

TED-AJ03-243

A PARAMETRIC STUDY ON SHAPE AND CROSS-SECTIONAL AREAS OF THE THIN FILM PRODUCED BY LASER CHEMICAL VAPOR DEPOSITION WITH A MOVING LASER BEAM

Yuwen ZHANG
Department of Mechanical Engineering
New Mexico State University
Las Cruces, NM 88003, USA
E-mail: yuwzhang@nmsu.edu

Keywords: Computational, Heat Transfer, Laser, Manufacturing, Vapor Deposition

ABSTRACT

Solid Freeform Fabrication (SFF) is an emerging manufacturing technology that directly creates three-dimensional parts from a CAD design. To produce fully functional structural components, gas based approaches to SFF such as Selective Area Laser Deposition (SALD) seem to be very promising. SALD utilizes Laser Chemical Vapor Deposition (LCVD) technique, which can be based on reactions initiated pyrolytically, photolytically or a combination of both [2], to deposit the film at the desired location on the substrate.

A Parametric study on shape and cross-sectional area of the thin film produced by LCVD with a moving laser beam is presented. The effect of natural convection on the LCVD process is neglected because it has little effect on the shapes of deposited film and has no effect on the cross-sectional area of the thin film. The problem is formulated in the coordinate system that moves with the laser beam and therefore, the problem is a quasi-steady state. The heat and mass transfer equations are

$$-\rho u_b \frac{\partial (c_p T)}{\partial x} = \frac{\partial}{\partial x}\left(k\frac{\partial T}{\partial x}\right) + \frac{\partial}{\partial y}\left(k\frac{\partial T}{\partial y}\right) + \frac{\partial}{\partial z}\left(k\frac{\partial T}{\partial z}\right) + S$$

$$-u_b \frac{\partial C}{\partial x} = D\left(\frac{\partial^2 C}{\partial^2 x} + \frac{\partial^2 C}{\partial^2 y} + \frac{\partial^2 C}{\partial^2 z}\right) + S_c$$

The governing equations with appropriate boundary conditions are solved numerically. The effects of laser scanning velocity, laser power and radius of the laser beam on the shapes of the deposited film are investigated. The results showed that a groove could be observed on the top of the film for higher laser power and lower scanning velocity. The cross sectional area, calculated by

$$A_c = \frac{2}{r_0^2}\int_0^\infty \delta dy$$

at different processing parameters is shown in Fig. A-1. It decreases with increasing scanning velocity. It also increases with increasing laser power and decreasing laser beam radius.

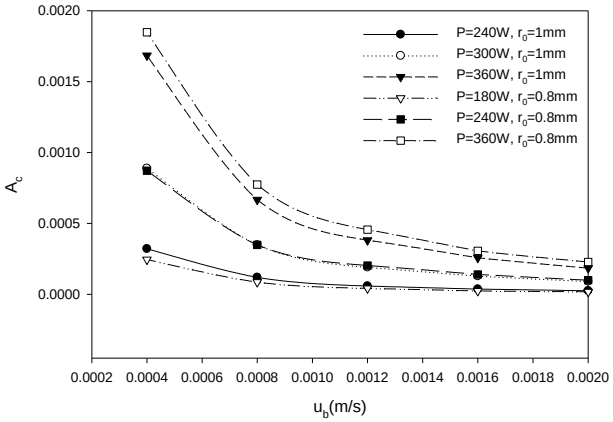

Fig. A-1 Dimensionless cross sectional area vs. scanning velocity

The following empirical correlation on the dimensionless cross sectional area is obtained.

$$A_c = a_0 + a_1\left(\frac{Bi}{Pe}\right)^{1.35}$$

where

$$a_0 = \begin{cases} -2.136\times10^{-5} + 6.126\times10^{-6}\,Bi & r_0 = 1mm \\ -9.206\times10^{-5} + 9.352\times10^{-5}\,Bi & r_0 = 1mm \end{cases}$$

$$a_1 = \begin{cases} 8.343\times10^{-7} + 1.423\times10^{-5}\,Bi & r_0 = 0.8mm \\ -2.587\times10^{-5} + 4.372\times10^{-5}\,Bi & r_0 = 0.8mm \end{cases}$$

NOMENCLATURE

A_c	dimensionless cross sectional area
Bi	Biot number
C	concentration (kg/m³)
c_p	specific heat (J/kgK)
D	mass diffussivity (m²/s)
E	activation energy (kJ/mol)
h	thickness of the substrate (m)
k	thermal conductivity (W/mK)
K_0'	Arrhenius constant
M	molecular weight (g/mol)
$\dot{m}$	mass flux (kg/m²)
P	laser power (W)
Pe	Peclet number
p	pressure (Pa)
q″	heat flux (W/m²)
r_o	radius of the laser beam (m)
R_u	universal gas constant (=8.314kJ/kmol)
S	source term in the energy equation
S_c	source term in the mass transfer equation
T	temperature (K)
x	coordinate in length direction(m)
y	coordinate in width direction (m)
z	coordinate in height direction (m)
Greek Symbols	
α	thermal diffusivity (m²/s)
α_a	absorptivity
γ	sticking coefficient
δ	thickness of the deposited film (m)
ΔH_R	heat of chemical reaction (J/kg)
ε	emissivity
ρ	density (kg/m³)
Subscripts	
g	gas
i	initial value
s	substrate
∞	infinite

INTRODUCTION

Solid Freeform Fabrication (SFF) is an emerging manufacturing technology that directly creates three-dimensional parts from a CAD design [1,2]. The SFF technologies that can build structurally-sounds parts are almost always powered by thermal fabrication of three-dimensional objects from powders or gases. To produce fully functional structural components, gas based approaches to SFF such as Selective Area Laser Deposition (SALD) seem to be very promising [3-5]. SALD utilizes Laser Chemical Vapor Deposition (LCVD) technique, which can be based on reactions initiated pyrolytically, photolytically or a combination of both [2], to deposit the film at the desired location on the substrate.

Mazumder and Kar [6] reviewed the theoretical and experimental works about LCVD up to 1995. More recently, Duty *et al.* have thoroughly reviewed materials, modeling and process control of LCVD [7]. Jacquot et al. [8] proposed a thermal model of the SALD process using acetylene (C_2H_2) as the source gas. Various phenomena, which included heat conduction in the substrate, chemical reaction during carbon deposition, and mass diffusion of acetylene in the chamber were taken into account. The temperature of the gases was, however, assumed to be uniform and therefore the heat transfer in the gas phase was neglected. Zhang and Faghri [9] developed a very detailed model of SALD process, which included the submodels of heat transfer, chemical reaction and mass transfer, and the model was employed to simulate the LCVD of TiN film on a finite slab with stationary and moving laser beams. The results showed that the effect of chemical reaction heat on the shape of deposited film was negligible.

Lee et al. [10] investigated the effect of natural convection on LCVD processes with stationary laser beams and concluded that the effect of natural convection of the gas on the thin film deposition rate was negligible. Zhang [11] investigated the quasi-steady state natural convection in LCVD process with moving laser beam. He found that the effect of natural convection on the shape of deposited film was negligible when the laser power was less than 300W. The shape of the cross-section of the film was slightly affected by natural convection when the laser power is 360 W. However, the cross-sectional areas obtained by the models with and without natural convection were almost identical even for higher laser power [11]. The numerical practices [11] indicated that inclusion of natural convection would significantly increase the CPU time to obtain the converged solution, which would prevent a thorough parametric study. For the purpose of parametric study, it is safe to neglect the effect of natural convection because it only has little effect on the shape of the deposited film and has no effect on the area of the cross-sectional area of the deposited film. In this paper, a thorough parametric study for LCVD with moving laser beams will be performed and an empirical correlation will be proposed.

PHYSICAL MODEL

The physical model of LCVD under consideration is illustrated in Fig. 1. A substrate made of Incoloy 800 with a thickness of h is located in the bottom of a chamber. Before the vapor deposition is started, the chamber is evacuated and then filled with mixture of H_2, N_2, and $TiCl_4$. A laser beam moves along the surface of the substrate with a constant velocity, u_b. The initial temperature of the substrate, T_i, is below the chemical reaction temperature, T_c. The vapor deposition starts when the surface temperature reaches the chemical reaction temperature. The chemical reaction taking place on the top substrate surface absorbs part of the laser energy and consumes the $TiCl_4$ near the substrate surface. The physical model of the LCVD process will include: heat transfer in the substrate and gases, chemical reaction, as well as mass transfer in the gases.

If the substrate is sufficiently large compared to the diameter of the laser beam, which has an order of magnitude of 10^{-3} m, a quasi-steady state occurs. The system appears to be in steady state from the stand-point of the observer located in and traveling with the laser

beam. Heat transfer in the substrate and gases is modeled as one problem with different thermal properties in each region [9, 11]. Since the model geometry is symmetric about the *xz* plane, only half of the problem needs to be investigated. For a coordinate system moving with the laser beam as shown in Fig. 1, the laser beam is stationary but the substrate and the chamber move with a velocity $-u_b$. The heat and mass transfer in the substrate and gases are modeled with the following equations:

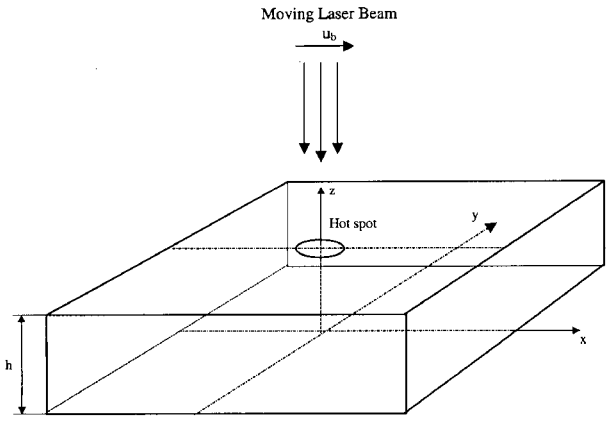

Fig. 1 Physical model

$$-\rho u_b \frac{\partial (c_p T)}{\partial x} = \frac{\partial}{\partial x}\left(k\frac{\partial T}{\partial x}\right) + \frac{\partial}{\partial y}\left(k\frac{\partial T}{\partial y}\right) + \frac{\partial}{\partial z}\left(k\frac{\partial T}{\partial z}\right) + S \quad (1)$$

$$-u_b \frac{\partial C}{\partial x} = D\left(\frac{\partial^2 C}{\partial^2 x} + \frac{\partial^2 C}{\partial^2 y} + \frac{\partial^2 C}{\partial^2 z}\right) + S_c \quad (2)$$

For the substrate region, the thermal properties are that of Incoloy 800, the substrate material. For the gaseous region, the thermal properties are determined by the individual thermal properties of H_2, N_2, and $TiCl_4$ as well as their molar fractions [9]. The source term in eq. (1) deals with the effects of laser beam heating and chemical reaction. The source term will be zero everywhere except at the substrate-gas interface under the laser spot. The heat flux at the substrate surface due to laser beam irradiation and chemical reaction is expressed as [11]

$$q'' = \frac{2P\alpha_a}{\pi r_0^2}\exp\left|-\frac{2(x^2+y^2)}{r_0^2}\right| - \varepsilon\sigma(T^4 - T_\infty^4) + \rho_{TIN}\Delta H_R u_b \frac{d\delta}{dx}, \quad z = h \quad (3)$$

where $d\delta/dx$ is the slope of the film thickness with respect to x, and is expressed as [11]

$$\frac{d\delta}{dx} = -\frac{\gamma_{TiN} K_0}{u_b \rho_{TIN}}\exp\left(-\frac{E}{R_u T_s}\right)C_s \quad (4)$$

where γ_{TiN} is sticking coefficient [11], and C_s represents the concentration of $TiCl_4$ at the surface of the substrate. The constant, K_0, in eq. (4) is defined as

$$K_0 = (C_{H_2})_i (C_{N_2})_i^{1/2} K_0' \quad (4a)$$

In order to use eq. (4) to determine the source term in eq. (1), the heat flux is treated as an internal heat source in the grid near the surface of the substrate.

The effect of the chemical reaction on the mass transfer is accounted for by a source term in eq. (2). The mass flux rate of $TiCl_4$ at the substrate is expressed as

$$\dot{m}_{TiCl_4} = -\rho_{TIN} u_b \frac{d\delta}{dx}\frac{M_{TiCl_4}}{M_{TiN}} \quad (5)$$

The source term in eq. (2) is then obtained by converting the mass flux of $TiCl_4$ into the mass source in the grid in gas phase immediately near the surface of the substrate.

The boundary conditions for eq. (1-2) are

$$T = T_i, \quad C = C_i \quad |x| \to \infty \quad (6a)$$

$$\frac{\partial T}{\partial y} = \frac{\partial C}{\partial y} = 0, \quad y = 0 \quad (6b)$$

$$T = T_i, \quad C = C_i \quad y \to \infty \quad (6c)$$

$$\frac{\partial T}{\partial z} = 0, \quad C = 0, \quad z = 0 \quad (6d)$$

$$\frac{\partial T}{\partial z} = \frac{\partial C}{\partial z} = 0, \quad z \to \infty \quad (6e)$$

NUMERICAL SOLUTION

The governing equations are written for the entire domain that includes both substrate and the gases. The concentration in the substrate region should be zero. The algebraic equations resulted from the control volume approach [12] have the following format

$$a_P \phi_P = \sum a_{nb}\phi_{nb} + b \quad (7)$$

By setting $a_p=10^{30}$ in eq. (7) at the grid point located in the substrate region for the mass transfer equation, zero concentrate field can be achieved [10]. The coefficients of the algebraic equations are altered before the algebraic equations are solved. The overall solution procedure is similar to that outlined in Ref. [9] and will not be repeated here. The typical number of iteration to get the converged solution is about 2000. In order to accelerate convergence, the initial temperature and concentration distributions for a specific case can be set as the converged temperature distribution for a similar case, which resulted in a reduction of the iteration number by 50% or more.

In order to simulate the LCVD in the moving coordinate system, the computational domain in x and y direction must be large enough so that the effect of the computational domain on the temperature and concentration distributions can be eliminated. The calculations were carried out for a non-uniform grid of 82 nodes in the x direction, 42 nodes in the y direction, and 82 nodes in the z direction. Finer grid sizes were also used in the calculations, but their results did not provide a noticeable difference with the present grid size.

RESULTS AND DISCUSSIONS

The code was validated by simulating heat conduction in the substrate with a moving laser beam [11]. The

steady state surface temperature obtained by numerical solution was compared with the temperature distribution caused by a moving point heat source [13]. The overall agreement between the two solutions was very good except at the locations near the center of the laser beam, which is due to the natures of heat sources modeled in analytical and numerical solution are different. The analytical result is for the temperature distribution caused by an infinitesimal heat source at *x=0*, while the numerical temperature distribution result is for a finite size heat source.

The numerical simulations of the LCVD process are performed with parameters similar to those in Ref. [11] but with broader range. The total pressure in the chamber is 207 torr and the partial pressure of Titanium Chloride is 7 torr. The partial pressures of N_2 and H_2 are the same. The thickness of the substrate is 5 mm. The radius of the laser beam, which is defined as the radius where the laser intensity is $1/e^2$ of the intensity at the center of the laser beam, is *0.8 ~ 1.0 mm*. The absorptivity of the laser beam at the substrate surface is taken to be 0.23 [6,14]. The activation energy of the chemical reaction is taken to be *E=51.02 kJ/mol*. The constant K_0, as defined in eq. (4a), is *8.4m/s*. Chemical reaction heat, ΔH_R, as determined by using JANAF thermochemical tables [15], is 5.379×10^6 *J/kg*. The initial temperature of substrate and gas is 338 K. The laser power varies from *180* to *360 W* and the scanning velocity ranged between *0.4* to *2 mm/s*.

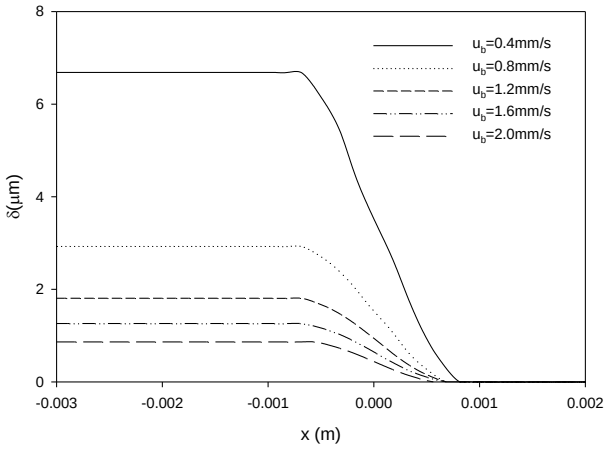

Fig. 2 Longitudal cross section of the deposited film (P=300 W, r_0=1 mm)

Figure 2 shows the cross sections of the deposited thin film at *y=0*. The scanning velocity varies from *0.4 mm/s* to *2mm/s*. The laser power is *300 W* and the radius of the laser beam is 1mm. It can be seen that the cross sectional area is not functions of x at locations in the wake of the laser beam, and the growth of the thin film only occurs in the spot directly under laser beam irradiation. The thickness of the thin film grows significantly with decreasing scanning velocity because the time of a particular spot exposed under laser beam increases with decreasing scanning velocity. The effect of laser scanning velocity on cross section of the thin film formed by LCVD process is shown in Fig. 3. The processing parameters in Fig. 3 are exactly same as that in Fig. 2. The thickness at the centerline of the thin film is highest when scanning velocity is higher than 1.2mm/s because the temperature at the centerline is highest. When the scanning velocity is less than 0.8mm/s, the top of the thin film become flat because the product of chemical reaction at the centerline cannot be fully stuck on the substrate [14].

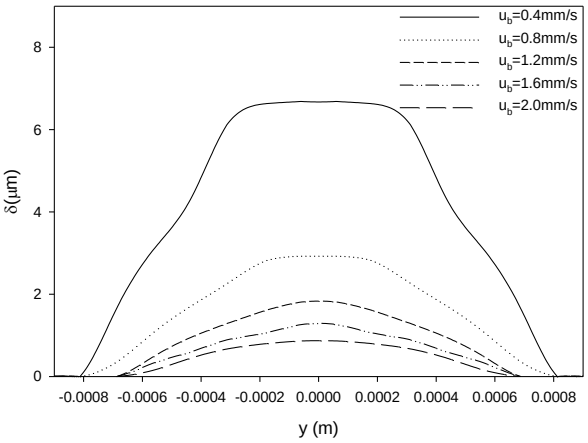

Fig. 3 Cross section (P=300 W, r_0=1 mm)

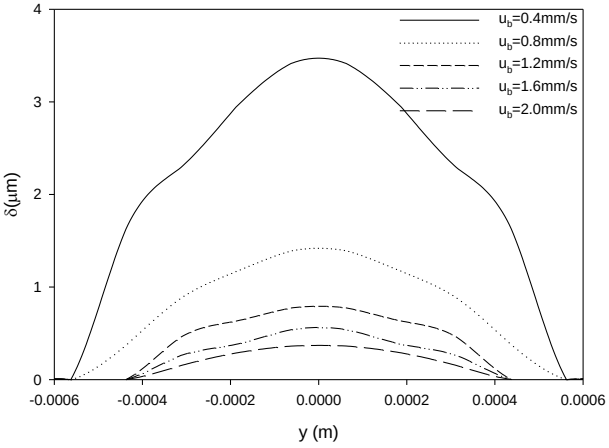

Fig. 4 Cross section (P=240 W, r_0=1mm)

Fig. 4 shows the effect of scanning velocity on the shape of the deposited film for a lower laser power (*P=240 W*). It can be seen that the flat top is not observed for all cases including u_b*=0.4 mm/s*. Fig. 5 shows the effect of scanning velocity on the shape of the cross-section of the deposited film at a higher laser power (*P=360 W*). The top of the thin film is flat for the cases of u_b*=1.6* and *2.0 mm/s*. When the scanning velocity is further reduced, a groove is observed on the top of the deposited film due to low sticking coefficient near the centerline. It is necessary to point out that while the flat top is desirable the SALD application but a deep groove on the top of thin film is not. Therefore, it is very

important to choose the processing parameters to get desirable shape of the cross section.

The numerical simulations are then performed for smaller laser beam radius and the results are shown in Fig. 6-8. The shapes of the deposited thin films for the laser power of *300 W* are shown in Fig. 6. The thickness of the film were significantly increased compared with the cases of r_0*=1 mm* because the decrease of the radius from *1* mm to *0.8* mm resulted in an increase of laser intensity by *56%.* The grooves are observed on the top of the film for all cases because higher laser intensity resulted in higher surface temperature and consequently lower sticking coefficient near the centerline of the thin film. Figure 7 shows the shape of the deposited thin film with a laser power of *240 W*. It can be seen that the shapes of the thin film for all cases, except for the case of u_b*=0.4 mm/s*, are similar to that of r_0*=1 mm* but the thickness of the film are significantly increased. For the case of u_b*=0.4 mm/s*, the top surface of the thin film is flat due to low sticking coefficient caused by higher surface temperature. Fig. 8 shows the shape of the deposited thin film with a laser power of *180 W*, which was not studied for r_0*= 1mm*. Grooves were not observed for all cases because the laser power is lower.

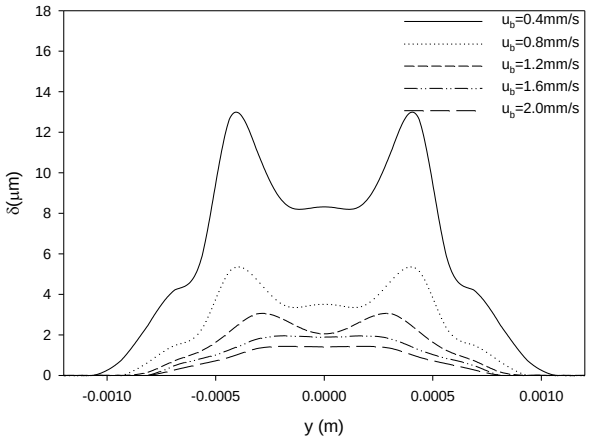

Fig. 5 Cross section (*P=360 W, r_0=1 mm*)

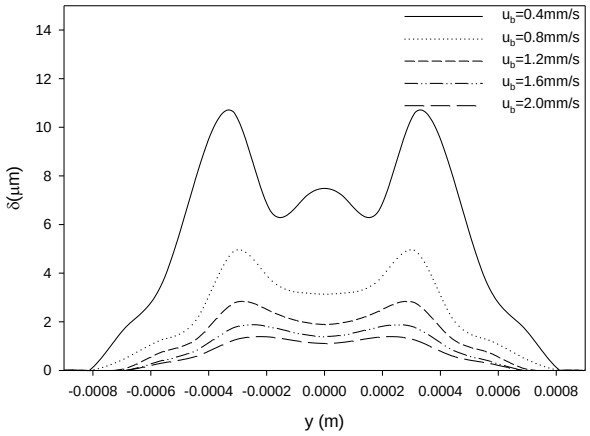

Fig. 6 Cross section (*P=300 W, r_0=0.8 mm*)

The variations of dimensionless cross sectional area with the laser scanning velocity at two different laser beam radii are shown in Fig. 9. The dimensionless cross sectional areas were obtained by

$$A_c = \frac{2}{r_0^2}\int_0^\infty \delta dy \qquad (8)$$

As can be seen, the cross sectional areas decrease with increasing scanning velocity. It also increases with increasing laser power and decreasing laser beam radius. In order to obtain empirical correlation for the dimensionless cross-sectional area, the results in Fig. 9 are replotted in Fig. 10. The dimensionless cross sectional area is plotted as function of Biot number and Peclet number, which are defined by

$$Bi = \frac{\alpha_a P}{\pi r_0 k(T_c - T_i)}, \quad Pe = \frac{u_b r}{\alpha} \qquad (9)$$

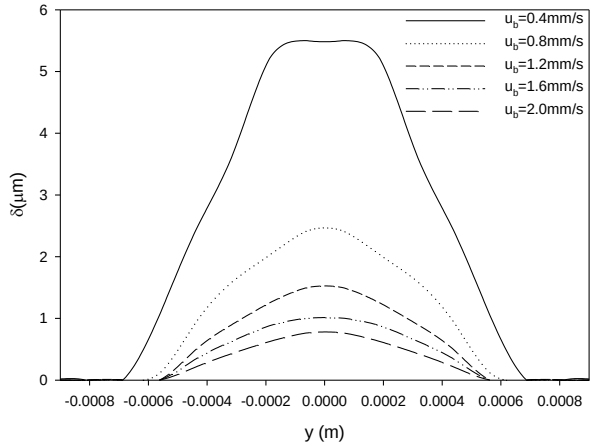

Fig. 7 Cross section (*P=240 W, r_0=0.8 mm*)

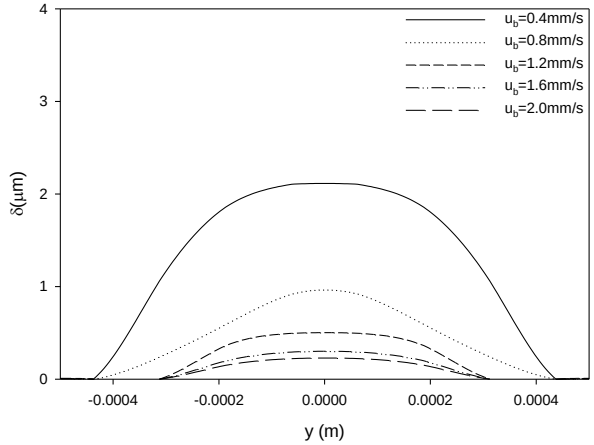

Fig. 8 Cross section (*P=180 W, r_0=0.8 mm*)

It can be seen that the dimensionless cross-sectional areas are linear functions of $(Bi/Pe)^{1.35}$ for all cases. The dimensionless cross sectional areas shown in Fig. 10 can be correlated into the following expression.

$$A_c = a_0 + a_1\left(\frac{Bi}{Pe}\right)^{1.35} \qquad (10)$$

where

$$a_0 = \begin{cases} -2.136\times10^{-5} + 6.126\times10^{-6}\,Bi & r_0 = 1mm \\ -9.206\times10^{-5} + 9.352\times10^{-5}\,Bi & r_0 = 1mm \end{cases}$$

$$a_1 = \begin{cases} 8.343\times10^{-7} + 1.423\times10^{-5}\,Bi & r_0 = 0.8mm \\ -2.587\times10^{-5} + 4.372\times10^{-5}\,Bi & r_0 = 0.8mm \end{cases}$$

The difference between the cross-sectional area obtained by numerical simulation and eq. (10) is less than 10%.

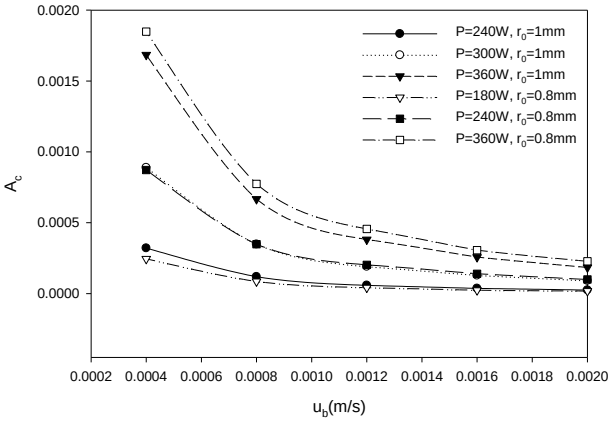

Fig. 9 Dimensionless cross sectional area vs. scanning velocity

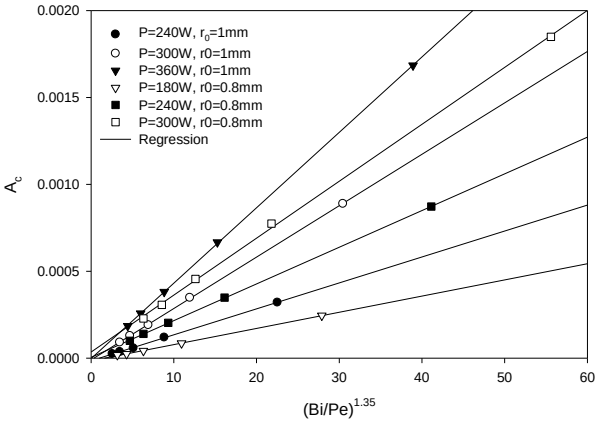

Fig. 10 Dimensionless cross sectional area vs. $(Bi/Pe)^{1.35}$

CONCLUSIONS

A parametric study on the LCVD of TiN film on a substrate with moving laser beam is presented. The effect of natural convection on the shape of deposited film is neglected because the effect on the shape and cross sectional area is insignificant. The results showed that a groove could be observed on the top of the film for higher laser power and lower scanning velocity. The cross sectional area decreases with increasing scanning velocity. It also increases with increasing laser power and decreasing laser beam radius. An empirical correlation on the dimensionless cross sectional area is obtained.

REFERENCES

[1] J.G. Conley and H.L. Marcus, Rapid Prototyping and Solid Freeform Fabrication, ASME *J. of Manufacturing Science and Engineering,* 119 (1997), 811-816.

[2] H.L. Marcus, G. Zong and P.K. Subramanian, Residual Stresses in Laser Processed Solid Freeform Fabrication, in *Residual Stresses in Composites: Measurement, Modeling and Effect on Thermomechanical Properties*, Edited by E.V. Barrera and I.Dutta, TMS, 1993.

[3] K.J. Jakubenas, B. Birmingham, S, Harission, J. Croker, M.S. Shaarawi, J.V. Tomkins, J. Sanchez, and H. Marcus, Recent Advances in SALD and SALDVI, *Procs. of 7th International Conference on Rapid Prototyping*, San Francisco, CA, March, 31-April 3, 1997.

[4] K.J. Jakubenas, Y.L. Lee, M.S. Shaarawi, H. Marcus and J.M. Sanchez, Selective Area Laser Deposition of Titanium Oxide, *Rapid Prototyping Journal*, Vol. 3, pp. 66-70, 1997.

[5] S. Harrison and H.L. Marcus, Gas-phase Selective Laser Deposition (SALD) Joining of SiC, *Materials and Design*, 20(1999), 147-152.

[6] J. Mazumder and A. Kar, *Theory and Application of Laser Chemical Vapor Deposition*, Plenum Publishing Co., New York, 1995.

[7] C.E. Duty, D.L. Jean and W.J. Lackey, Laser Chemical Vapor Deposition: Materials, Modeling, and Process Control, *International Materials Reviews*, 46(2001), 271-287.

[8] Y. Jacquot, G.-S. Zong and H.L. Marcus, Modeling of Selective Laser Deposition for Solid Freeform Fabrication, *Proceedings of Solid Freeform Fabrication Symposium,* 1995, 74-82.

[9] Y. Zhang and A. Faghri, Thermal Modeling of Selective Area Laser Deposition of Titanium Nitride on a Finite Slab with Stationary and Moving Laser Beams, *Int. J. Heat Mass Transfer*, 43(2000), 3835-3846.

[10] Y.L. Lee, J.V. Tompkins, J.M. Sanchez and H.L. Marcus, Deposition Rate of Silicon Carbide by Selected Area Laser Deposition, *Proceedings of Solid Freeform Fabrication Symposium 1995*, 433-439.

[11] Y. Zhang, Quasi-Steady State Natural Convection in Laser Chemical Vapor Deposition with a Moving Laser Beam, *Proceedings of 2002 International Mechanical Engineering Congress and Exposition*, New Orleans, LA, Nov. 17-21, 2002.

[12] S.V. Patankar, *Numerical Heat Transfer and Fluid Flow*, Hemisphere, Washington, DC, 1980.

[13] Carslaw, H.S., and Jaeger, J.C., *Conduction of Heat in Solids*, Clarendon, Oxford, 1959.

[14] O. Conde, A. Kar and J. Mazumder, Laser Chemical Vapor Deposition of TiN Dot: A Comparison of Theoretical and Experimental Results, *J. Applied Physics,* 72 (1992), 754-761.

[15] W.M. Chase, JANAF Thermochemical Tables, 3rd

Edition, *J. Phys. Chem. Ref. Data* 14 (1986), Suppl. 1.